

# Indoor localisation of a mobile agent using prototype based techniques

Robert M. Bwana

**Abstract**—The adoption and use of mobile agents relies on the ability to determine their positions. While mobile agents in outdoor environments can make use of GPS systems or topographic imaging, indoor mobile agents may not be able to reliably do so. This research sets out to investigate the potential of mobile agents to determine their indoor position without the use of any extra marking or assisting technologies.

I attempt to determine locality using dimensionality reduction and mapping algorithms to map information inherent in the working environment to the location of the mobile agent. While many linear and non-linear mapping algorithms are available, my research, outlining one of two approaches taken, focuses on using the Self-Organised Neighbour Embedding (SONE) algorithm and the Self-Organised Map (SOM) algorithm. These had been proven in prior research to successfully map higher dimensional data to determine locality in lower dimensional space.

The approach would focus on using wireless local area network signal strengths which the mobile agent would be able to measure with pre-existing inbuilt capabilities. This wireless signal information was gathered over a period of 2 weeks at an industrial warehouse representing real world usage scenarios.

The results of the research suggest that while the wireless signal data does indeed contain information which could be of use in indoor localisation, the 2 unsupervised learning algorithms used were not sufficient to overcome the inherent noise in the data. This would indicate that semi-supervised or probabilistic embedding methods could yet manage to successfully map the wireless signal information onto the lower dimensional geographic space.

**Index Terms**—Localisation, Neighbourhood embedding, SONE, SOM, Mobile Agent.

---

## 1 INTRODUCTION

Mobile agents, such as flying drones, need to be able to determine their location. The majority of mobile agents do this in 2 primary ways: using GNSS signals, or relying on user input.

The Global Navigation Satellite System (GNSS), which includes systems such as the Global Positioning System (GPS), relies on line-of-sight communication between the mobile agent and satellites located in varying orbits around the earth to calculate and determine the position of the mobile agent.

Relying on user input in essence requires a human element of input. The mobile agent would rely on the human user being aware of the relative position of the mobile agent to him-/herself and use this as input into any system that may require it.

Both of these two approaches come with limitations.

Firstly, the use of GNSS relies on minimal interference between the satellites and the mobile agent and while this may be achievable with mobile agents in an outdoor environment, this is not the case with indoor applications.

Secondly, relying on user input requires a human to be present and attentive at all times throughout the operation of the mobile agent. While this may be acceptable in certain circumstances, it does limit the capacity to automate the tasks of the mobile agent.

In this report, an alternative method of localisation is outlined, explained, tested, and reported on. This method of localisation is intended for indoor environments which aim to use mobile agents in some autonomous or semi-autonomous manner whereby the mobile agent is capable of determining its location and thereby allowing other events to occur based on this information.

Such an approach uses the wireless signals emitted by wireless network access points present in indoor environments. More specifically,

the signal strength of the signals emitted from each wireless access point is considered in order to determine the location of the mobile agent.

Such an approach would be ideal as it would not necessitate the installation of any proprietary equipment and would take advantage of infrastructure and installations assumed to be already present in most indoor environments, i.e. wireless networks. Were this to be realised, it would be reasonable to assume that it would be a cost-efficient manner of enabling indoor localisation of mobile agents when compared to alternatives.

The mobile agent would merely have to move around the environment, likely initially under supervision, in order to gather the necessary wireless signal information. After this, it would train itself based on the gathered data and learn through the algorithms a manner to determine its location in the geographic environment.

This would be done through the creation of a radio-map i.e. a mapping of radio waves onto an actual geographic location.

Real world data is used in this research and indoor localisation is unproven for the warehouse environment in which this research is based. For these reasons, two algorithms are used so that the results of each can be compared with one another. Should both algorithms provide suitable results it can be determined that the data gathered is suitable for the task at hand while should one algorithm be suitable while the other is not, it can be determined that a particular algorithm is better suited at the task at hand over the other. Should both algorithms not provide suitable results, it may be necessary to consider that the data gathered is not suitable to carry out the task of indoor localisation in its current form.

For this research the Self-Organised Neighbour Embedding (SONE) algorithm as well as the Self-Organising Map (SOM) are used to attempt to find a lower dimensional representation of the wireless data in order to be able to determine the lower dimensional location based on the higher dimensional wireless signal.

Other linear algorithms

It should be noted that what actions are taken based on the location of the information is outside the scope of this research, it is only necessary to determine the possible locations of the mobile agent based on the received wireless signal strengths.

The remainder of this paper is organised as follows: in section 2,

- 
- R.M. Bwana is a MSc Computer Science student at the University of Groningen, E-mail: r.m.bwana@student.rug.nl.
  - This work was carried out in collaboration with Ankita Dewan, who investigated localisation using t-SNE.

the data acquisition process is described followed by data cleaning and preprocessing in section 3. Section 4 and 5 introduce the two algorithms to be used for this research. The descriptive statistics of the data gathered are thereafter presented in section 6 as well as some initial investigation into the data. Section 7 then explains the experimental set up while sections 8 presents the results of the two algorithms. This paper is concluded in section 9 as well as suggestions provided for future work.

## 2 DATA ACQUISITION

Our validation environment was an area of 900 square meters in the warehouse building such that four aisles (named, ZA-ZB-ZC-ZD) were covered. In the span of two weeks of collection, two aisles (ZB,ZC) were getting loaded and unloaded as a part of daily operation, one aisle (ZA) was always empty and one was always filled (ZD).

Data was acquired at two levels : through equipment and manually.  
**A. Data acquired through the equipment** : Parrot Bebop 2 drone quad-copter device was used to capture signal and in-flight information, and images and videos as well. The navigation controls were possible through a specialized software run on standard laptop as well as through a dedicated smartphone app. The former was used for our project wherein the drone and computer communicated over standard WiFi connection. While the long range of Bebop 2 and built-in calibration features provided much reliability, several inconveniences were experienced with respect to the drop in connectivity, sometimes leaving the drone stranded in mid-air or continuing to move in a fixed direction.

The section under study contained Access Points (AP) that transmit the signals from ceiling over entire area underneath. Specialized software, developed by the drone owners, was used to capture signal measurements as Received Signals Strength Indication (RSSI) values. A total 505 positions were used by performing at most three height measurements at intermittent distances along the four aisles. At every position, approximately 20 readings were taken for fingerprinting based positioning which marks potential improvement in accuracy scores.[8]. Every reading was stored in json format with a number of fields.

**B. Data acquired manually** : Laser measurements were taken manually at each of the 505 positions to maintain labels for potential use later during algorithm development/evaluation. Length measurements were taken with reference to a wall adjoining the first aisle, ZA. Breadth measurements were taken along the aisle taking one end as reference. For height measurements, readings were made against the floor. Below is the range of physical dimensions in which the project was carried out :

Length : 0m-12.25m [Wall till aisle ZD]

Width : 0m-56.5m [Aisle beginning till aisle end]

Height : 0m,1m and 1.5m

The central walking space between every two aisles is approx 1.5m. The distance between central points of any two aisle is approximately 3m.

Data acquisition is the first step for developing indoor navigation methods and suffers from shortcomings that may propagate later into the development phase. It was not straight-forward to determine if the accuracy of drone and the complex enclosed environment were complementing forces or otherwise. Data quality assessment was not entirely plausible and movement of drone was the only way to judge the quality of data being collected. Therefore, the challenge during data collection was to control the drone accurately and efficiently to maintain the desired distance and orientation with respect to the selected positions. A small portion of overall data still contained noisy indoor data especially at locations where disturbances during drone in-flight were noted because of external matters as below :

a.) The warehouse ceiling lightning system was motion controlled.

With switching off of the lights due to lack of movement by people in the various had direct impact on drone's flight and on data acquisition leading to possible data inconsistencies for a few locations.

b.) Due to the size of the warehouse as well as its internal layout, small wind currents and drafts formed quite frequently within it. This had an adverse impact on the flight of the drone as well as its stability.

c.) Aisle ZA was filled with boxes covered with black tape and it was noted that the drone would repel away from such containers, slightly deviating from the actual navigation path.

d.) This was also the case with black paint or dark markings on the floor of the aisles. This caused the drone to fluctuate along the vertical axis whenever it encountered such markings on the floor.

e.) From the total number of days spent in collecting data with the drone, there were some days when aisle ZD and ZC were loaded with boxes containing marshmallows. In this case, it was noted that weaker signal strengths were captured by the drone, as evident from table 2. Signal strength ranges (in dBm) for the overall strongest emitters are compared for regularly filled aisle ZB and marshmallow filled aisle ZD (case of signal attenuation)

BSSID	Aisle ZB	Aisle ZD (with marshmallow)
54:3D:37:2A:8E:F8	36-39	45-49
54:3D:37:0E:D3:E8	37-40	36-39
24:C9:A1:00:65:68	42-46	44-48
54:3D:37:6A:8E:F8	31-40	44-50

All the problems related to drone's movement were addressed to some extent by enabling the drone's calibration feature during its flight and by manual inspection of drone positioning.

Data in certain locations were missing completely as they were not recorded while at the warehouse.

The locations ZA001 up to and including ZA007 were sealed off due to water collecting on the floor. This was considered a potential environmental hazard to human operators walking on it and any electronic equipment that would need to be placed on it. Readings from ZA009 onwards were collected as normal.

ZD.L065.H0 was not recorded due to unfortunate circumstances. The battery of the drone was depleted during recording the measurements and was replaced just after. No information was written to a file at that position, a fact unfortunately only noticed once the data was being cleaned.

## 3 PREPROCESSING

After gathering the data, it was deemed necessary to pre-process the data before it could be used in subsequent steps. The data gathered contained missing values, fields which weren't required for the algorithms, and features which was felt would not greatly contribute to the performance of the algorithm which could be discarded to improve the algorithm's runtime. The pre-processing involved data cleaning, treating data missingness and finally preparing data in a format that could be easily given as input to the algorithm.

### 3.1 Feature extraction

As stated earlier, json files with in-flight information were created for every position that the drone was stalled at and at least 20 json files were produced at every position. The original set of field values collected by the equipment were:

- Time : Every json file is uniquely marked by the time field information.

- Yaw : Right and left rotation
- Pitch : Forward and backward lean
- Roll
- Speedx, speedy, speedz
- Altitude : Altitude information is necessary but laser measurements are used instead.
- Signal network : Signal names
- BSSID : Unique set of signal ids which were used all through the project for analysis and algorithm development.
- Signal Strength : Integer values reported in the range of (-100,0) in unit of decibels relative to 1 milliwatt (dBm) for every BSSID at identified by the drone at every location for various time-stamps.
- Channel : Number of controls (yaw,pitch,throttle,roll) for movement

For the current project, BSSID and signal strength were of main use and therefore, after data collection the json files were altered to store only the two fields. Time-stamps were also of relevance, as shall be discussed in next section of missingness, and were retained for pre-processing steps.

### 3.2 Data representation

Using python scripts, a data frame was created with fingerprints (represented by multiple json files at every physical location) as rows and BSSIDs as columns. Table 1 shows a sample set from the data-frame. Signal strength values were populated into the data structure wherever the values were available from drone captured data and the remaining were kept blank at this stage. For cases where more than one measurements were recorded for the same BSSID and at the same time-stamp, the average values were assigned in the data frame.

### 3.3 Cleaning and missingness imputation

A total of 88 BSSIDs were captured by the drone but 17 BSSIDs were later found to be corrupted with alphabets appended to original BSSIDs during data inspection. For example :- records with BSSID : 24:C9:A1:40:65:68bcmwl were corrected to BSSID : 24:C9:A1:40:65:68.

Based on the cleaned data it was observed that through the duration of the data acquisition phase of the project, wireless signals from 71 unique sources were observed and recorded. Apart from distinguishing strong signals from the weak signals, analysis was also conducted based on percentage availability of the signals. In theory, the percentage availability plays a significance role because signals that are more frequent and a high percentage availability may result in biasing and infrequent or sporadic signals may result in outlier cases. In either cases the results could be affected because from the entire warehouse only a smaller section was considered as the experimental setup, hence a smaller sample space.

Records relating to all 71 of these features had missing values within them ranging from features with less than 0.5% missingness to features with close to 100% missingness, that is, features that were detected only once throughout the entire data gathering period. This was assumed to be from other mobile wireless network devices such as laptops or PDAs which are used around the warehouse. It was therefore decided to select only features that appeared somewhat consistently throughout the data. Figure 1 shows the 71 features sorted according to the completeness. The x-axis label is not that of

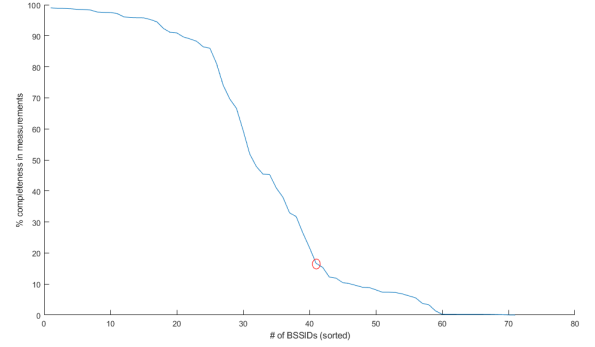


Fig. 1: Sorted percentage completeness values of all 71 BSSIDs to determine threshold percentage completeness

the feature number, but rather the number of features up to that point.

An elbow point was taken at feature 41 which had a completeness of 16.67%, indicated in Figure 1 by a red circular marker point. The 41 most complete features were therefore carried forward for use in training the models with the remaining 30 no longer considered.

Last value carried forward method was adopted for missing data imputation because our application has time-series data wherein value prediction is possible based on history values at a location. At location 'L', when signal 'X' is received by the drone at time-instant 'T', it can help predict the signal strength that the drone would have recorded at time-instant 'T + t' if the signal 'X' had been successfully captured at the same location during the new time-instant. The carry forward was performed for a.) fingerprints at a location and b.) one location to the next such that they were in the same aisle and not so far away within the same aisle. Table 1 shows a few signal strength records before imputation and table 2 shows the filled in values that were eventually used for further steps in the project. The approach, while justified on basis of the nature of signal strengths, was still prone to resulting in values that look worse than they would truly have been.

	00:1F:9D	24:C9:A1	24:C9:A1	24:C9:A1
ZAL009H0.1	NaN	NaN	-76	-72
ZAL009H0.2	NaN	NaN	-77	-72
ZAL009H0.3	NaN	NaN	-77	-72
...	...	...	...	...
ZAL119H0.6	-85	-91	-73	-77
ZAL119H0.7	-86	NaN	-72	-70
ZBL001H0.1	NaN	NaN	-66	NaN
ZBL001H0.2	NaN	NaN	-75	-65
ZBL001H0.3	NaN	NaN	-75	-65
...	...	...	...	...
ZDL119H1.5.5	NaN	NaN	-67	-73
ZDL119H1.5.6	-84	-83	-68	-55
ZDL119H1.5.7	NaN	NaN	-71	-72

Table 1: Before imputation

## 4 SONE

Self-Organised Neighbour Embedding (SONE), was originally introduced in literature as Neighbourhood Embedding - Exploratory Observation Machine (NE-XOM) as outlined in [1].

This defines the cost function:

$$E_{\text{SONE}} = \int \sum_i \delta_{\Psi_D(s), x^i} \cdot \sum_j D \left( h_{\sigma}^{\Psi_D(s)}(j) \parallel g_{\xi}^s(j) \right) p(s) ds$$

	00:1F:9D	24:C9:A1	24:C9:A1	24:C9:A1
ZAL009H0.1	-90	-90	-76	-72
ZAL009H0.2	-90	-90	-77	-72
ZAL009H0.3	-90	-90	-77	-72
...	...	...	...	...
ZAL119H0.6	-85	-91	-73	-77
ZAL119H0.7	-86	-91	-72	-70
ZBL001H0.1	-90	-90	-66	-90
ZBL001H0.2	-90	-90	-75	-65
ZBL001H0.3	-90	-90	-75	-65
...	...	...	...	...
ZDL119H1.5.5	-75	-81	-67	-73
ZDL119H1.5.6	-84	-83	-68	-55
ZDL119H1.5.7	-84	-83	-71	-72

Table 2: After imputation (NaNs replaced with last carried forward values)

where  $\Psi^D(s)$  for  $(S)$  is defined as:

$$\Psi^D(s) = x^i \text{ such that } \sum_j D \left( h_{\sigma}^{\Psi^D(s)}(j) \parallel g_{\gamma}^s(j) \right) \text{ is minimum}$$

The SONE algorithm relies on 2 neighbour coefficient parameters referred to as  $\sigma$  (sigma) and  $\gamma$  (gamma).  $\sigma$  represents the neighbourhood coefficient in the higher dimensional space while  $\gamma$  represents the neighbourhood coefficient in the lower dimensional space.

The SONE algorithm, when used for localisation, can be summarised as an iteration of the following few steps:

1. Calculate pairwise dissimilarities
2. compute the neighbourhood co-operations
3. for each data item
  - (a) draw a random position
  - (b) determine winner based on dissimilarity
  - (c) compute the neighbourhood functions
  - (d) update the embedding in the lower dimension based on the rule:

$$y^k = y^k - \epsilon \Delta y^k$$

with  $\epsilon$  representing the learning rate.

The pairwise dissimilarities used was the euclidean distance measure. This results in the dissimilarities between two data points  $d_{i,j}$  being reflexive, i.e.  $d_{i,j} = d_{j,i}$ . While other dissimilarity measures are feasible and were considered, it was decided to remain with the euclidean distance measure of dissimilarity.

## 5 SOM

The second algorithm tried was the Self-Organising Map (SOM) also referred to as the Kohonen Network [4, 5]. While the SOM algorithm has been demonstrated by Kohonen to cluster documents [7, 6, 3], this has not limited its use in other use cases [5, 10, 2].

The SOM algorithm relies on the relation between a node in the higher dimensional space node and its mapping to a point in the lower dimensional space. In the higher dimension determining similarity of the input to a node using a dissimilarity measure and then updating the winning node as well as nearby nodes. The update is calculated using the learning rule:

$$m_i(t+1) = m_i(t) + h_{ci}(t)[x(t) - m_i(t)] \quad (1)$$

where  $h_{ci}$  represents the neighbourhood function determining how much the nearby nodes  $i$  are updated when node  $c$  is the winning node [7].

For this research the lower dimensional space would represent a position on the warehouse floor while the higher dimensional points would be compared to the wireless signal data.

The dissimilarity measure used by the SOM algorithm chosen was once again the euclidean distance as in the SONE algorithm. This was to avoid any possible bias of a dissimilarity measure to the data.

## 6 DESCRIPTIVE ANALYSIS

RSSI is a measure of power level that the mobile agent receives from the access point and distance between the two objects determines strength of the signal received in combination with the surrounding environment conditions. Signal strength values in the range (-100,-60) dBm are regarded as poor strength measures as that's the situation when signal is drowning in the surrounding noise. The optimal and practically attainable range is (-50,-20) dBm. The analysis of signal strength measurements depends on the choice to remove noise signals before missingness imputation or before algorithm application. In the current project, missingness is treated first, followed by analysis being performed over all measurements and then the qualitative observations made during analysis are used to filter out noisy (poor) measurements before the main algorithm is executed.

### Measures of spread in the data

The combined raw data had a mean of -65.4617 dBm, median of -65 dBm, and a standard deviation of 12.4219 dBm. Figure 2 shows a box-plot indicating the means and measures of spread of the 71 individual BSSIDs.

As can be observed, a majority of BSSIDs have a recorded mean between -50 dBm and -80 dBm. The BSSIDs with a mean value of around or below -90 dBm coincide with those with a high degree of missingness, as shown in Figure 3. We therefore conclude these to be the BSSIDs of boundary access points which were at a distance to the data collection area so as to only be detected in certain circumstances and be absent otherwise. Despite using two differing algorithms to try and create an accurate lower dimensional representation of the wireless data, as neither of them succeeded it was decided to investigate the data further to determine whether the problem lay with the data. The investigation into the data began with an investigation into the PCA values which were used as input for the algorithms.

### PCA investigation

Figure 4 shows the 2D PCA output colour coded to represent the positions as introduced in Figure 13.

As can be observed from Figure 4, even when represented by the 2 most principal components i.e. the 2 components representing the largest variance in the data, there is still a degree of overlap in the data. This would, in naive attempts at clustering, result in highly inaccurate classifications.

Furthermore this reinforces the conclusion that the measurements between positions are similar to one another. This would pose a challenge to the embedding algorithms.

To get a glimpse into the spread within individual aisles, the points representing only the individual aisles in the PCA output were plotted in turn. The PCA outputs of the individual aisles are shown in Figure 5 for aisle ZA, Figure 6 for aisle ZB, Figure 7 for aisle ZC, and Figure 8 for aisle ZD.

From the figures, it can be observed that certain aisles had a greater spread than others as is the case with aisle ZD when compared with aisle ZA, the two extremes.

As the intensity, read darkness, of the colour gradually increases or decreases based on the proximity of the point it represents to the end of the aisle we can then observe from Figures 5 to 8 that positions within the aisles can also be differentiated within certain confidences. While not perfectly gradual in terms of colour intensities, the spread of colour intensity in the figures suggest that sections within the aisles can be, to some extent, distinguished from other sections within the same aisle.

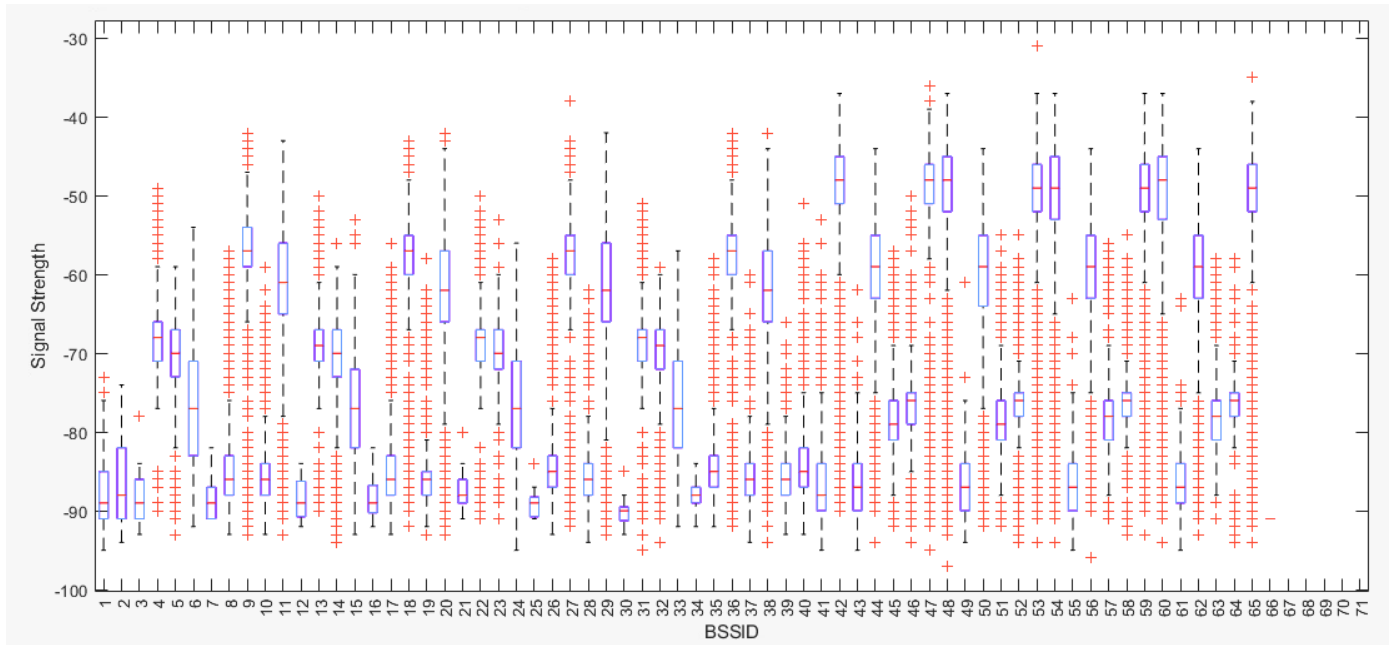


Fig. 2: Boxplot indicating mean and spread values of signal strengths of all 71 BSSIDs. The BSSIDs with mean signal strength around or below -90 dBm are noted and looked up in Figure 3 to determine pattern, if any.

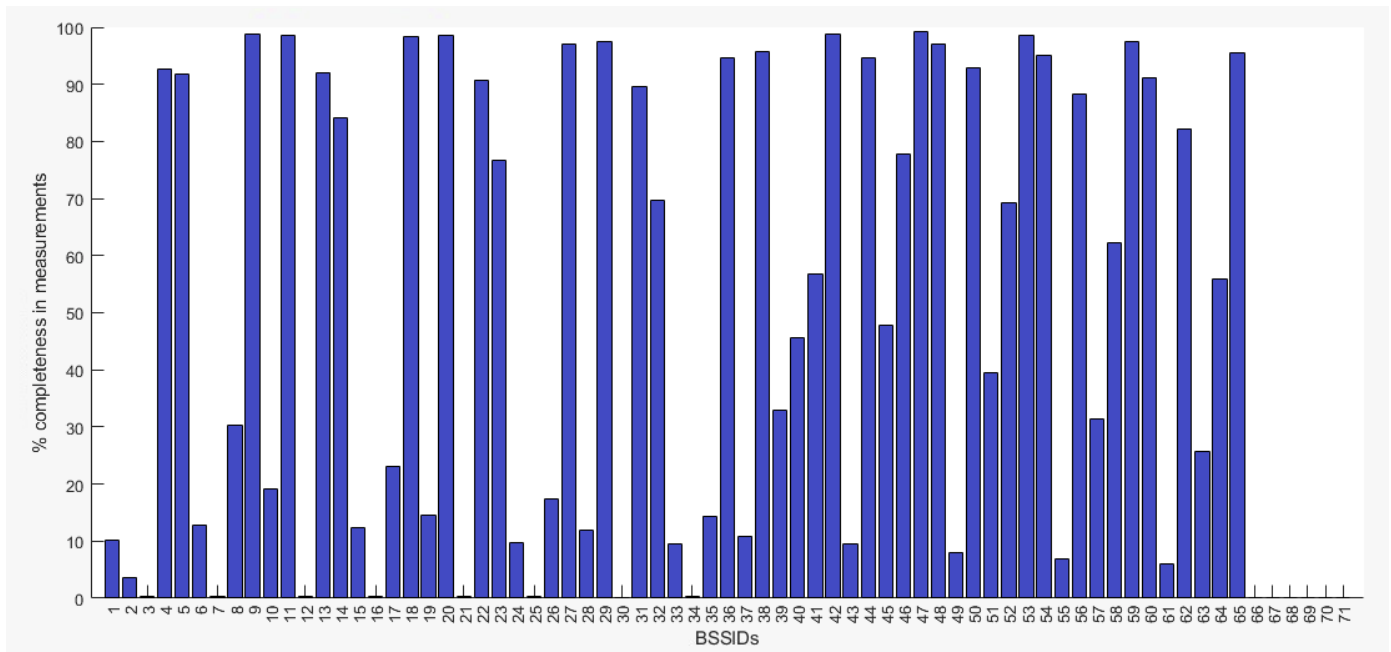


Fig. 3: Bar-plot indicating percentage completeness per BSSID to investigate potential correlation between low mean signal strength values (from Figure 2) and high degree of missingness).

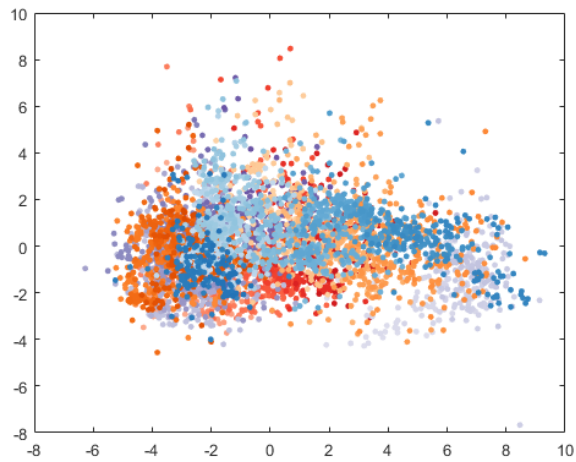


Fig. 4: The data points after PCA translation, colour coded based on position.

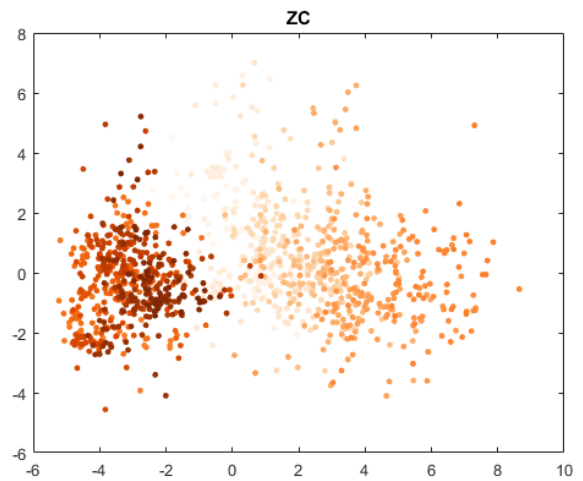


Fig. 7: PCA mapping of the positions in aisle ZC. While there is a large separation within the lighter shades, the darker shades of orange appears confined to a smaller space.

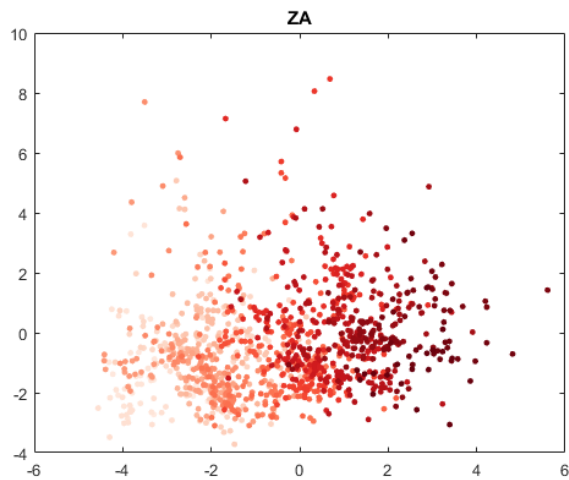


Fig. 5: PCA mapping of the positions in aisle ZA. The separation between the lighter and darker colours indicate a reasonable spread in the data.

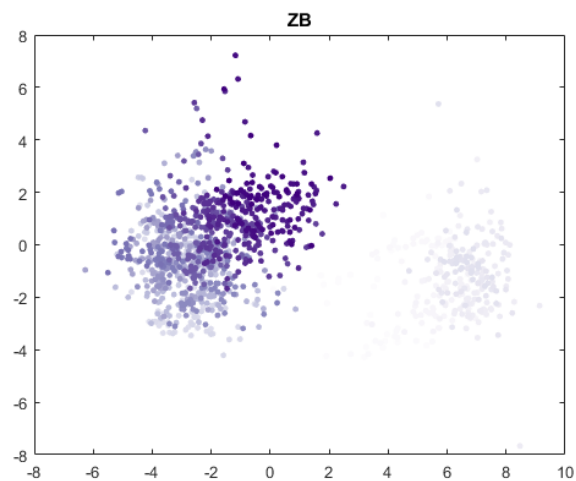


Fig. 6: PCA mapping of the positions in aisle ZB. A large separation of data is observable.

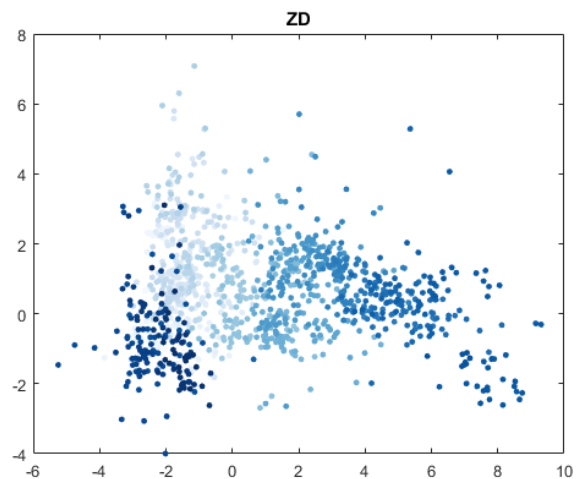


Fig. 8: PCA mapping of the positions in aisle ZD. While the data is well separated regarding the shades of blue, the darkest blue is closest in proximity to the lightest blue, a less than ideal situation.



It can therefore be argued that once the mobile agent can determine in which aisle it is currently located, it would be able to distinguish with some degree of accuracy how far along the aisle it currently is. The challenge appears to be then, as Figure 4 shows, that the variation between the aisles makes it a challenge to differentiate which aisle it currently inhabits.

This could be due to the range of the dimensions in question. The distance from one end of an aisle to the other covers a span of 56.5 meters, while the distance between the aisles located furthest apart from each other (ZA and ZD) covers a distance of only 10.5 meters.

### Nearest Neighbour Investigation

Following the PCA investigation, a simple Nearest-Neighbour investigation was performed. The intention of this was to see how often, for each point, it's neighbouring points belong to the same geographic position as it. This would assist in determining whether data points representing the same position do tend to appear within an acceptable distance of one another.

For this investigation, the 10 data points with the smallest euclidean distance to the data point in question were compared and a simple first-past-the-post voting system was conducted.

Such a voting system caters for cases where there may be no clear majority and there are more than 2 classes (in this case positions) which could be voted for. In such cases the class with the highest number of votes is considered the winning class.

This was repeated for all 4700 recorded data records (20 records per position with 235 positions in question), with the results per position combined.

It was observed that the majority of points were either correctly classified or classified as adjoining points. Out of the 235 positions only 2 locations were incorrectly classified as not even adjacent positions. There was no discernible reason as to why they were classified as such.

The outcome of the nearest neighbour investigation, caused us to believe that the data gathered can indeed be useful in the localisation of the mobile agent, but that the accuracy obtainable is limited as the data has more points which neighbour dissimilar points rather than those belonging to the same class.

## 7 EXPERIMENTAL SET UP

In order to use the data gathered, it was necessary to normalise the data.

The data was z-score transformed per feature, that is:

For feature  $i = 1, \dots, 41$  :

For all values of feature  $i$ :

$$x = \frac{x - \mu_i}{\sigma_i}$$

The z-score transformed values were used as input into both algorithms.

As the number of records collected per position varied from one position to another, it was decided that a limited number of points would be taken from each position to prevent positions where a greater number of values were recorded from having an outsized influence over others. The limit was set to a maximum value of 20 records per position with this number reduced when quick tests were conducted to refine parameters. This limit ensured that all positions had an equal number of records.

### 7.1 SONE experimental set up

For initial\_y's, the Principal Component Analysis (PCA) was performed with the 2 most principal components taken as initial y points. The algorithm was run for 400 epochs.

Due to the steps and calculations performed in the algorithm, all data values were multiplied by a constant value of 1000 so as to be able to deal in integer values exclusively.

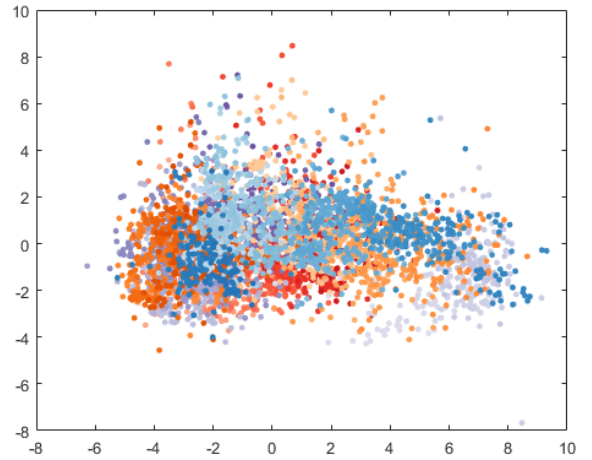


Fig. 9: Initial positions of data points (colour coded per actual position). This was used as input into the SONE algorithm.

The parameters were annealed from a starting value for  $\sigma$  of 10 down to 0.5 and from 20 to 1 for values of  $\gamma$ .

For the learning rate,  $\epsilon$ , the starting value was 0.5 which was annealed down to 0.05 over the 400 epochs.

### 7.2 SOM experimental set up

The SOM algorithm used during this research was that which was implemented in the inbuilt `nctools` Neural Network toolkit on MATLAB for a simple exploration of the data and then the `SOM-Toolbox` for MATLAB provided under the GNU General Public License by Esa Alhoniemi, Johan Himberg, Jukka Parviainen and Juha Vesanto for more in depth analysis.

As with the SONE algorithm, the z-score normalised values were used as input into the SOM algorithm. The lower dimensional grid was structured having dimensions of 4 x 60, with each node representing a floor grid position.

## 8 RESULTS

In this section, the results from both algorithms are presented independently at first. Finally a comparison between the two sets of results is made.

### SONE Results

For initial tests, a square grid was used as the lower dimensional structure to see whether the points would group together without any structuring aspect to the lower dimensional positions.

The resulting positions are shown in Figure 10.

As can be observed, the positions are more spread out than the initial positions shown in Figure 9. Furthermore, the spread in positions result in loose groupings of same or similar colouring indicating that some similarities are picked up by the algorithm and appropriately shifted together.

Despite this, there does not appear to be enough separation to differentiate the individual positions in clusters or as would be the most ideal; if they formed the structure of the aisles.

To see whether structuring the lower dimensional grid in a shape resembling the floor of the warehouse, 2 grids were created with dimensions representative of those to the floor plan of the warehouse. Each of the 2 grids represent a situation where the floor is aligned with either the first principal component or the second. The algorithm was then run using each grid in turn.

The reason for aligning the lower dimensional grid with the first principal component is that this component represents the greatest variation of data and therefore may be the best fit in terms of the longest dimension of the grid.

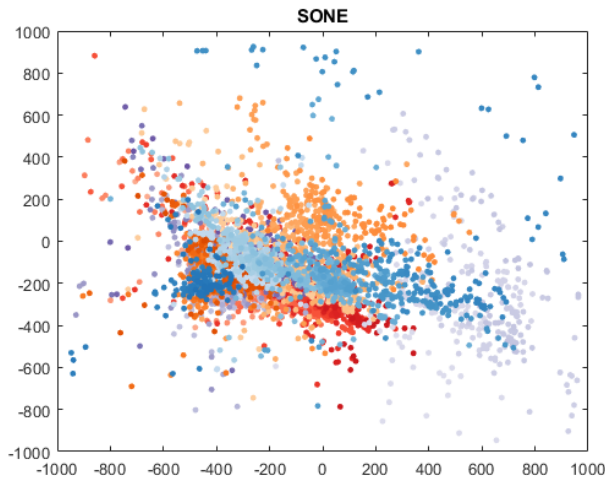


Fig. 10: SONE output positions of data points. A good separation of the periphery points but large cluster in the centre still not separated.

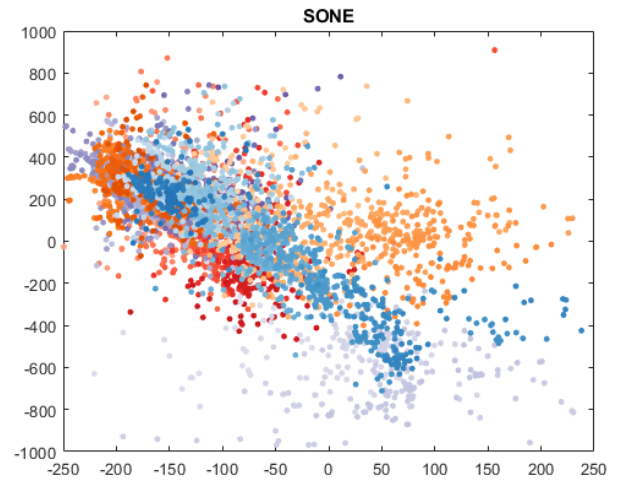


Fig. 12: SONE output based on grid aligned with 2nd principal component. A better separation of the orange colour-coded positions, but a large part of the central block is still not separated.

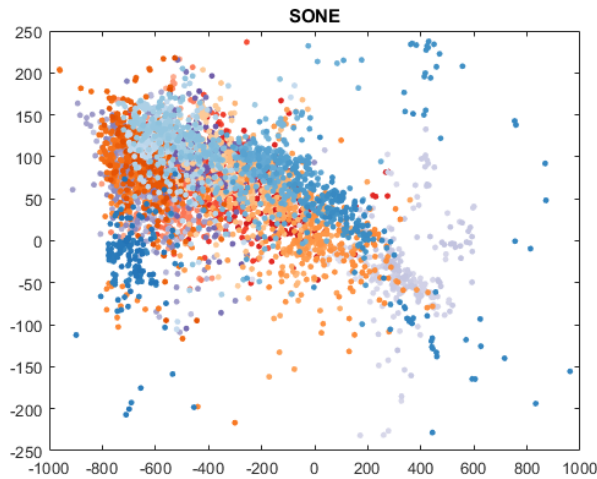


Fig. 11: SONE output based on grid aligned with 1st principal component. While the central bulk has been shifted, it has not been better separated.

Figure 11 shows the SONE output based on the grid aligned with the first principle component.

While the output differs from that shown in Figure 10, a number of the same clusters are found. The clusters are restricted in how far away from each other they separate along the vertical axis, as a product of the vertically restricted underlying structure. Unfortunately, it fails to provide a clearer separation of the large 'central mass' of data points than prior solutions.

A second directed grid aligned with the second principal component was tried. The reason for trying this is to test whether applying an element of rotation to the data would assist in separating the final positions achieved.

Figure 12 shows the SONE output based on the grid aligned with the second principal component.

From initial impressions it does appear that some clusters are better separated. The large light orange cluster of points towards the higher x-values are better separated from the 'central mass' of data points than with any other underlying structure attempted so far. The red cluster at the lower y-value area of the 'central mass' of points also appears to be better separated from the 'central mass' of points than



Fig. 13: Ground truth colour representation of points.

prior attempts.

Nevertheless, none of the attempts to apply SONE to the unstructured data proves to be successful in clustering the data in the lower dimensional space in a manner which represents the ground truth.

## SOM Results

Figure 14 shows the final winning classification for each position in the lower dimensional space. This is relative to the ground truth values as shown in Figure 13. The ground-truth colour scheme was chosen in order to allow the distinct differentiation between aisles and gradual differentiation of points within the same aisle.

It can be observed from Figure 14 that the winning class i.e. position based on the trained map can spill over the aisles and deviates in a number of areas quite drastically from the ground truth.

The results indicate successful grouping of similar positions in the same area, but unfortunately these are at the wrong actual positions.

## 8.1 Comparison of results

With the small difference in the way the two algorithms approach the lower dimensional mapping, the difference in their results must be taken into perspective.





Fig. 14: Winning classification of position based on number of hits. While a number of groupings appear, the difference with the ground truth is noticeable.

As SOM bases its lower dimensional positions on a provided grid structure, the alignment of positions with one another cannot be compared to the alignment of the positions produced by SONE.

Furthermore while SOM updates the higher dimensional nodes based on distance to one another, SONE updates the lower dimensional mappings based on the two neighbourhood functions decreasing the likelihood that the final positions will be perfectly aligned.

While ideally the output positions of SONE would align with the grid introduced as input to SOM, this would represent a perfect scenario unlikely to be obtained without perfect data.

It is therefore only possible to observe how positions are voted by SOM in respect to one another and compare them with how the output produced by SONE structures the positions with respect to one another.

The SOM output shown in Figure 14 shows the groupings of similar data with one another, incorrectly in terms of what their final positions should be. However one can observe the same grouping of data shown in the SONE output as shown in Figure 12 especially in terms of how these groupings locate with respect to one another.

This would indicate that both algorithms can identify similar wireless signal information but the difficulty seems to lie in aligning this to the lower dimensional space.

## 9 CONCLUSION

In conclusion, despite best efforts, the pursuit to create a lower dimensional representation of the wireless data which accurately reflected the ground truth was unsuccessful.

Despite having real world data and using multiple algorithms, the results obtained while showing some initial promise, proved to be unsuccessful in accomplishing the task at hand.

The research project, which this report describes, was carried out as a full start-to-finish data science and machine learning project. From the initial data gathering plan through all the various stages described within to the writing of this report and an accompanying presentation, the project was intended as an opportunity to gain real-world expertise and put into practice what had previously been learnt in academic environments. This aspect of the research was a success.

## Future work

There exists several opportunities to improve upon or expand upon this research.

A design decision made when carrying out this project was to treat the wireless signal readings as unstructured data in the algorithm. While helping with the simplicity of the algorithm the data can also be interpreted and analysed in a structured manner. As mentioned when justifying the missingness imputation, subsequent values in the readings can be assumed to correlate with the values in the readings taken just prior to them. This works on the basis that as the mobile agent moves closer to- or further away from- the source of the wireless signal, the signal strength will improve or degrade respectively in a non-random manner. With this in mind, a future area of research would be to take advantage of the structure within the data in determining the location of the mobile agent.

Another area of research that could be investigated in the future would be to take advantage of a combination of data sources produced by the mobile agent. This, of course, depends on the mobile agent in question, however were a flying drone similar to the one used for this research be available, various sources of information could be used such as the images taken from the drone's camera. This could be used to assist the results of the radio-map based algorithms to determine not only the position of the mobile agent, but its proximity to objects or barriers which could better inform its localisation.

## REFERENCES

- [1] K. Bunte, F.-M. Schleif, S. Haase, and T. Villmann. Mathematical foundations of the self organized neighbor embedding (sone) for dimension reduction and visualization. In *ESANN*. Citeseer, 2011.
- [2] G. Deboeck and T. Kohonen. *Visual explorations in finance: with self-organizing maps*. Springer Science & Business Media, 2013.
- [3] S. Kaski, T. Honkela, K. Lagus, and T. Kohonen. Websom—self-organizing maps of document collections1. *Neurocomputing*, 21(1-3):101–117, 1998.
- [4] T. Kohonen. Self-organized formation of topologically correct feature maps. *Biological cybernetics*, 43(1):59–69, 1982.
- [5] T. Kohonen. The self-organizing map. *Proceedings of the IEEE*, 78(9):1464–1480, Sep 1990.
- [6] T. Kohonen, S. Kaski, K. Lagus, J. Salojärvi, J. Honkela, V. Paatero, and A. Saarela. Self organization of a massive document collection. *IEEE transactions on neural networks*, 11(3):574–585, 2000.
- [7] K. Lagus, T. Honkela, S. Kaski, and T. Kohonen. Self-organizing maps of document collections: A new approach to interactive exploration. In *KDD*, volume 96, pages 238–243, 1996.
- [8] H. Leppäkoski, S. Tikkinen, and J. Takala. Optimizing radio map for wlan fingerprinting. *2010 Ubiquitous Positioning Indoor Navigation and Location Based Service*, pages 1–8, 2010.
- [9] P.-O. Persson and G. Strang. A simple mesh generator in matlab. *SIAM Review*, 46(2):329–345, 2004.
- [10] A. Ultsch and H. P. Siemon. Kohonen's self organizing feature maps for exploratory data analysis. In B. Widrow and B. Angeniol, editors, *Proceedings of the International Neural Network Conference (INNC-90), Paris, France, July 913, 1990 I. Dordrecht, Netherlands*, volume 1, pages 305–308, Dordrecht, Netherlands, 1990. Kluwer Academic Press.